THE PROPERTIES OF WING AND AIRFLOW OF FLYING INSECTS

Koji TSUYUKI , Seiichi SUDO
Department of Mechanical Engineering, Iwaki Meisei University

Keywords: *Biomechanics, Flapping flight, PIV, Wing morphology*

Abstract

This paper describes the results of some experiments concerning wing morphology and flight performance of several flying insects; cicadas, dragonflies and bumblebees. Firstly, the surface shapes of three insect wings were visualized by a distinct three-dimensional image. The surface shapes showed a difference of functions for flapping flight between each wing. Secondly, the distribution of velocity fields around a flapping dragonfly, a flapping bumblebee and a flapping cicada were visualized with a PIV system to identify the airflow generated by the wings. Periodical vortex rings were observed in the result with the bumblebee. Finally, the successful observation of a flapping cicada the free flight is reported.

1 Introduction

Insect flight has especially fascinated a lot of scientists and the flight mechanisms of various insects have been investigated extensively [1-4]. The studies of flapping flight have contributed to developments in biomechanics and bioengineering. For example, a flapping flight robot has been developed as an application [5, 6]. Although these have been a lot of research on insect flight, further research is required for developments in biomechanics and bioengineering to continue. There still remain unexplored domains concerning the mechanisms of flapping flight. For instance, the properties of insect wing and airflow around flapping insects have generally remained unresolved because of the large number of insects that exists. Each insect has different flight mechanics. If we study more about insect flight, the results of such studies will lead to further developments in the biomechanics and bioengineering. To this end the current paper investigates the airflow around several flapping insects. In this paper, we visualized and examined some three-dimensional images of several insect wings and the airflow around three different flapping insects. The results of these experiments are described.

2 Experimental Apparatus and Procedures

2.1 Three-dimensional Surface Roughness of Insect Wings

The surface roughness of an insect wing was measured by the three-dimensional curved shape measuring system [7]. Figure 1 shows a schematic diagram of the experimental apparatus for the measurement of an insect wing. This measuring system was composed of a microscope system, a laser displacement detector system, an automatic high accuracy scanning X-Y stage system, and an automatic focusing system. A curved shape measurement of a sample wing was performed to the submicron accuracy. And we found the measuring system was suitable for the observation of the surface roughness of insect wings to the minutest of details. The sample wing was severed from the insect body before the start of the measurement, and it was mounted on the X-Y stage. After the severing, the wings of the in-

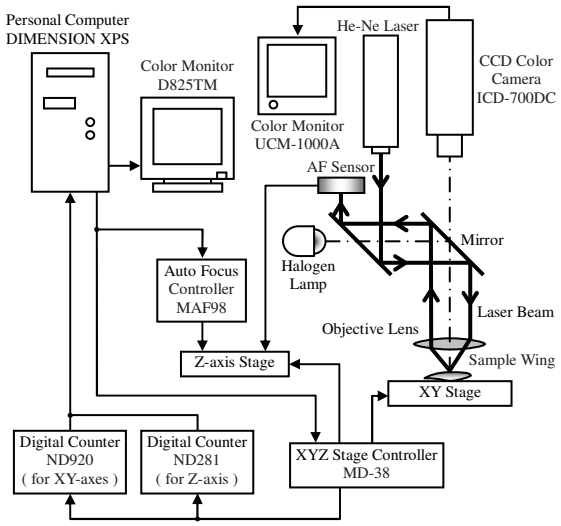

Fig. 1 The experimental apparatus for the measurement of three-dimensional surface roughness of an insect wing

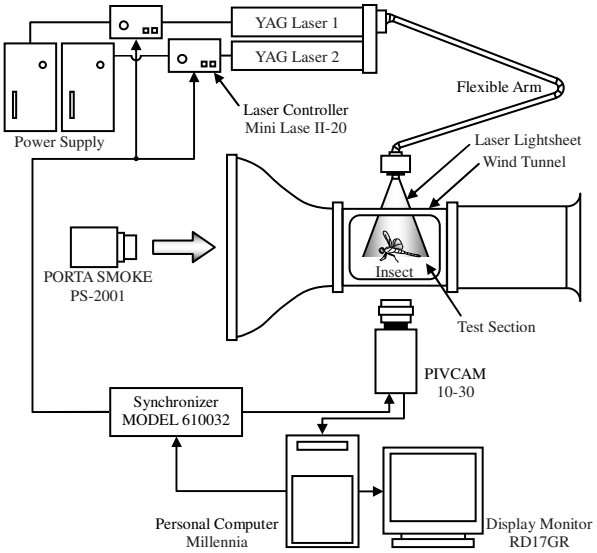

(a) PIV system with small wind tunnel

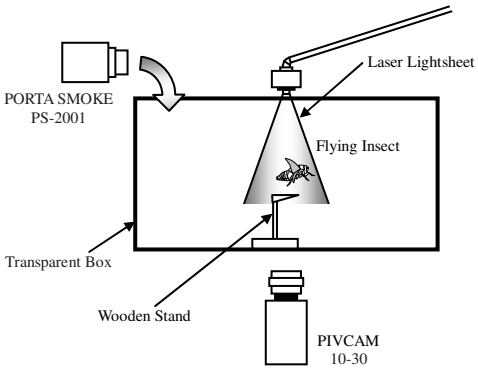

(b) Cicada in transparent enclosed box

Fig. 2 The experimental apparatus for the measurement of velocity fields around an insect

sects were coated with gold using an ion sputtering method in order to catch the reflection of the laser beam. This was necessary because insect wings mostly consist of transparent membranes. When a laser beam hits the surface of the sample wing, a diffused or scattered reflection occurs. The scattered light reflection is then focused through an objective lens on a unique semiconductor sensor. An output signal from the photodetector gives the position of the measured surface relative to a gauge probe. The three-dimensional measurement of the whole surface of the sample wing is made by autoscanning the wing with the X-Y stage and processing these images with a computer. The surface roughness of a dragonfly, cicada and bumblebee were measured using this experimental system.

2.2 Velocity Fields around Flapping Insects

A lot of papers investigate the visualized flow fields around flapping insects [8-10]. However, there are few papers that analyze and observe flapping insects using by a Particle Image Velocimetry (PIV) system. The PIV system was established for the measuring two-dimensional flow fields. Therefore, we have used the PIV system to reveal the characteristics of airflow around flapping insects. Figure 2 (a) shows a schematic diagram of the experimental apparatus. The flapping insects were analyzed by using the PIV system in a small wind tunnel. This experimental system was composed of a CCD camera, a small low-turbulence wind tunnel, two Nd: YAG lasers, a synchronizer, and a personal computer. The test section of the wind tunnel was 200 mm high, 200 mm wide and 300 mm long. The turbulence intensity at the test section was 0.75 % rms at velocity $U_0 = 10$ m/s. Each test insect was fixed in a

uniformly smooth wind field in the test section of the wind tunnel. The insect was tethered for measurement. The velocity fields during the wing flap of a dragonfly and bumblebee were measured by the experimental system.

The measurement of velocity fields around a free flight cicada was also performed using the PIV system without the small wind tunnel. The cicada was mounted on the wooden stand in the transparent enclosed acrylic box shown in Fig. 2 (b). This box was 400 mm high, 400 mm wide and 800 mm long. The height of the wooden stand was 115 mm, and the stand was set at near the center in the box. The measurement of velocity fields was performed at the moment of taking off.

3 Experimental Results and Discussions

3.1 Three-dimensional description of surface roughness of the insect wings

In general, insect wings do not have a flat surface. For instance, a large roughness of the cross section along the costa was identified on the wing structure of a dragonfly. Moreover it is well known that this structure contributes to the good performance of dragonfly flight [11]. Even though the cross sections of insect wings are quite complex in structure, there are very few studies describing the roughness of insect wings. This complex structure has not yet been shown to exist for all insect wings. So, we measured the surface roughness of three different insect wings, the dragonfly, bumblebee, and cicada wings in order to reveal the wing structure of these insects. And we also compared the surface roughness of each wing. In the measurement, total values of the height of undulation at each cross section were minimized by setting the insect wing on the X-Y stage.

3.1.1 Three-dimensional image of the dragonfly wing

Figure 3 shows the three-dimensional surface roughness image of the right forewing of the dragonfly, *Sympetrum frequence*. The body length of the dragonfly was $L = 39.81$ mm, the right forewing length was $l_f = 32.51$ mm. The color indicator in this figure displayed the height of undulation on the wing. The display of the forewing has been separated into eight pieces for the observation of seven cross sections. Though the figure was cut into eight pieces, the color indicator was put on the surface before the wing was separated. It can be seen that the leading edge to the trailing edge formed a big camber near the center region. The dragonfly generates aerodynamic lift by using this center region of the wing [12]. Furthermore, it can be observed that the thick veins made a large undulation with a V-shaped like groove moving from the root of the forewing along the leading edge. There was a small undulation near the tip of the forewing. Therefore, each section of the dragonfly wing performs different functions. Figure 4 shows the relationship between the non-dimensional wing length and the non-dimensional undulation of two different kinds of dragonfly wings. Even though the dragonfly wings are shown the transition tendency of the undulation is same. Dragonflies in the suborder *Anisoptera Selys* commonly have the same undulation in wings morphology. That is, the root of the wing strongly and flexibly supports the wing, the center of wing creates the lift force through the big camber and the wingtip keeps the airflow under control for steady flight.

3.1.2 Three-dimensional image of the cicada wing

The three-dimensional surface roughness image of the right forewing of the cicada, *Tanna japonensis japonensis* is shown in Fig. 5. The color indicator was put on the surface before wing was separated as in Fig. 3. The body length of the cicada was $L = 25.92$ mm, the right forewing length was $l_f = 36.22$ mm. Cicadas are usually heavier than other insects, as such the cicada wing needs to be larger to generate enough lift force. While dragonflies have the V-shaped groove near the leading edge of their wings cicada do not. There was no prominence of undulation on the cicada wing, however there is a

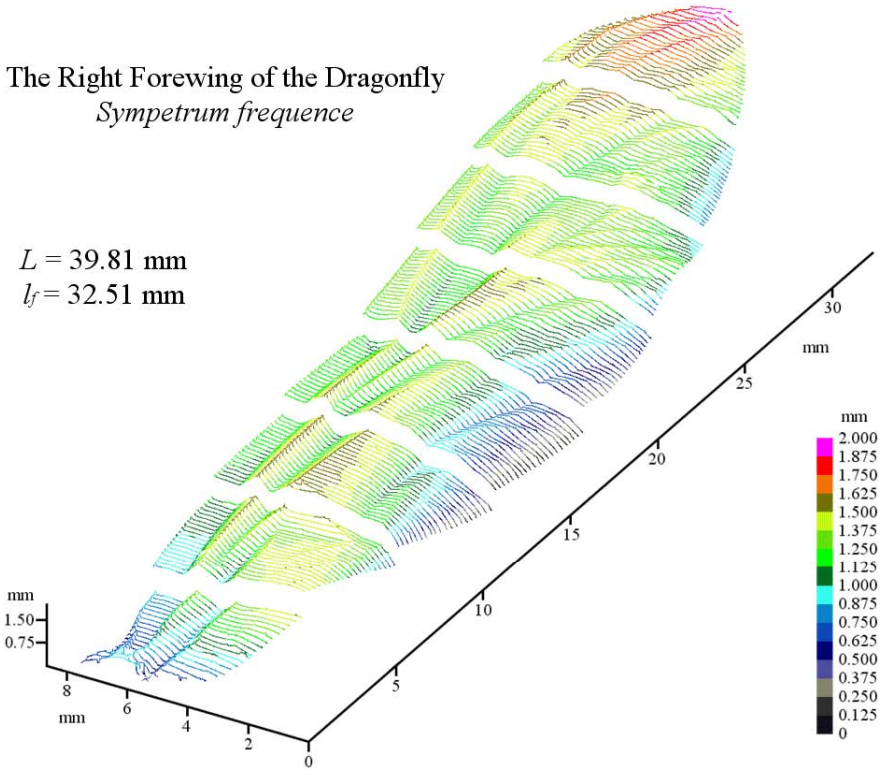

Fig. 3 The right forewing of the dragonfly, *Sympetrum frequence*

corrugated surface to about 20 mm from the root of the forewing as in shown Fig. 6. Figure 6 (a) shows a cross section of the dragonfly from the root to the wingtip, and Fig. 6 (b) shows a cross section of the cicada from the root to the wingtip. It can be seen that the cross sections are different between the dragonfly and the cicada. This corrugated surface could be responsible for the unique shape of the cicada riblet. Furthermore, there is a camber from 15 mm to about 25 mm on the forewing shown in Fig. 5. These properties of the cicada wing seem to suggest that each wing part has different functions for flight. We believe that these structures combine to control airflow over the whole wing to ensure smooth and powerful flight.

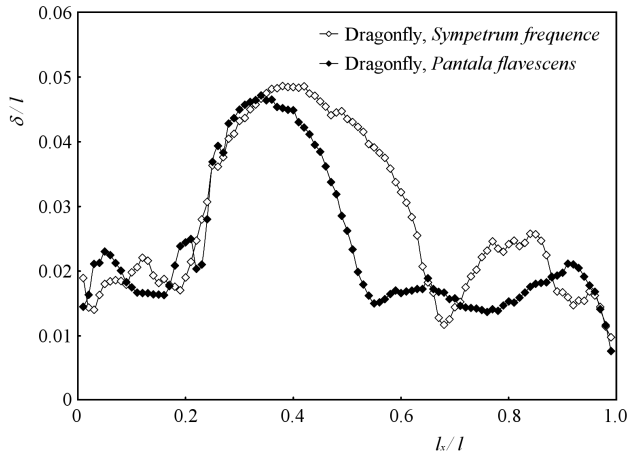

Fig. 4 The distribution of the non-dimensional undulation on the dragonfly wings

3.1.3 Three-dimensional image of the bumblebee wing

Figure 7 shows the three-dimensional surface roughness image of the left forewing of bumblebee, *Bombus diversus diversus*. The body length of the bumblebee was $L = 16.20$ mm, the right forewing length was $l_f = 13.36$ mm. It can be observed that the high position of the forewing was at the wingtip near the leading edge. In general,

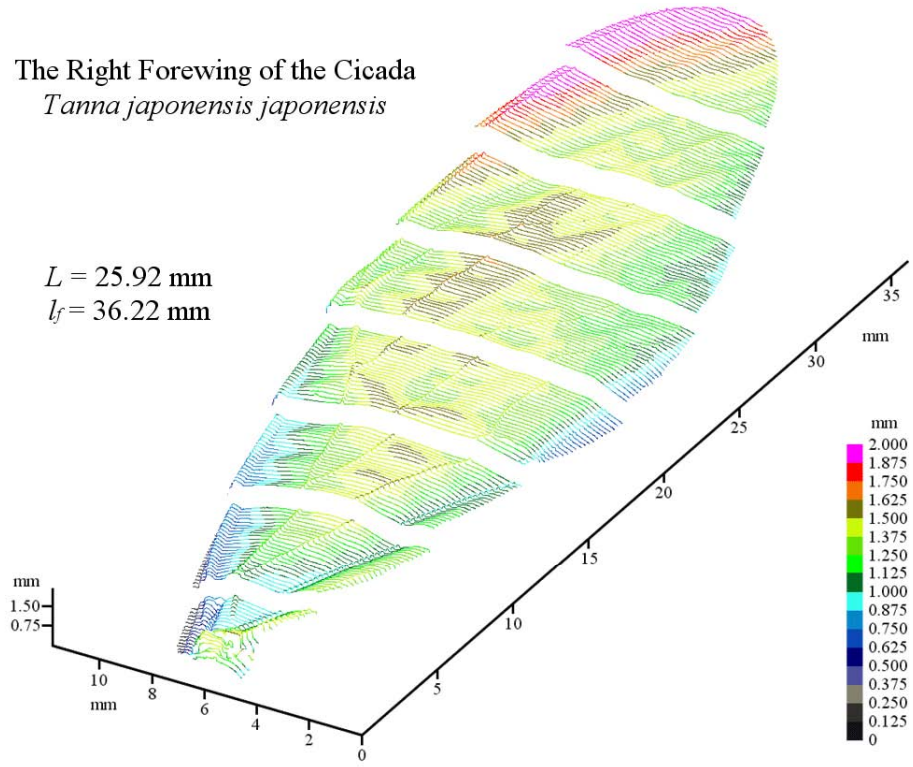

Fig. 5 The right forewing of the cicada, *Tanna japonensis japonensis*

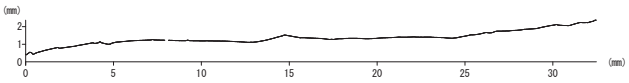

(a) The dragonfly, *Sympetrum frequence*

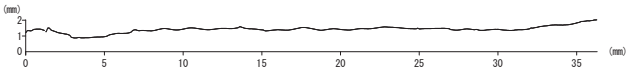

(b) The cicada, *Tanna japonensis japonensis*

Fig. 6 The sample of cross sections from the root to the wingtip

a bee connects its forewing with its hindwing by hooks called 'hamuli' on the leading edge of the hindwing during flapping flight. The photomicrography of the hamuli of a bumblebee, *Bombus ardens ardens* is shown in Fig. 8. As such, we have measured the three-dimensional surface roughness image of the forewing connected with the hindwing of the bumblebee. Figure 9 shows the measurement result of the same bumblebee. It is important to note that when the forewing and the hindwing were connected the high position of the wing shifted from the leading edge of the forewing to the hindwing as shown in Fig. 9. That is, these results suggest that the forewing has to connect with the hindwing to make flapping flight possible for bumblebees.

Wing shape has important relevance to flapping flight. That is to say those characteristics of surface roughness on the wing of the dragonfly, cicada, and bumblebee indicate that each insect has a different mechanism for flight performance and airflow around its wings.

3.2 Velocity vectors around the flapping insects

Flow visualization around insects has been studied by many scientists. For example, Dickinson

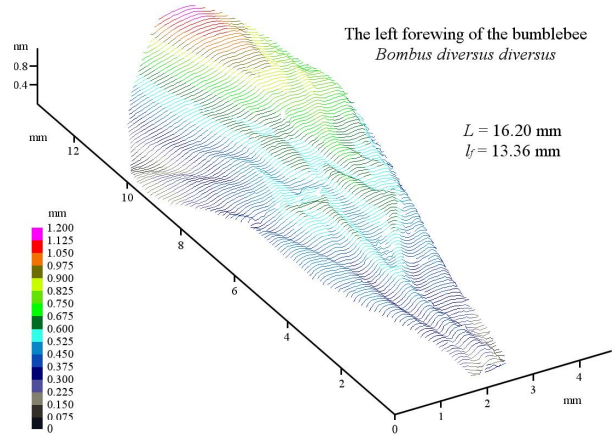

Fig. 7 The left forewing of the bumblebee, *Bombus diversus diversus*

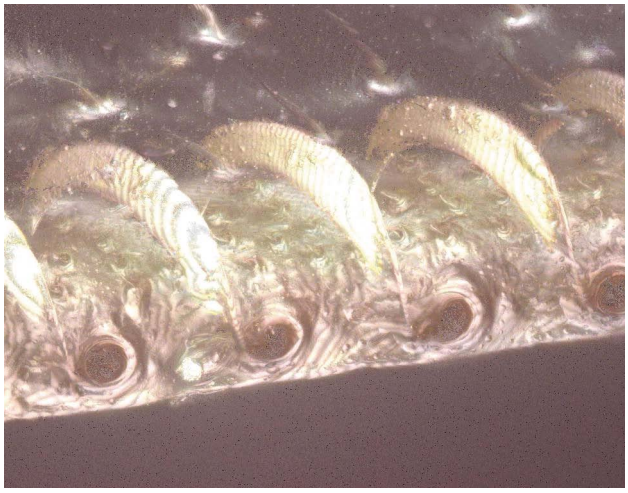

Fig. 8 The microscope photograph of the hamuli of the bumblebee, *Bombus ardens ardens*

and Gotz [10] studied the dynamics of force generation during the flight of fruit flies out of a visualized airflow around the fruit flies. Fearing *et al.* [5] measured the flow field around a fruit fly using the PIV system for making a micro-robot. However, there has not been enough researches to fully reveal the flapping flight mechanism.

We now understand that insect wings have different shapes and functions as mentioned above. That is, the flight mechanism for each insect is different. Therefore, we have analyzed velocity vectors around the flapping flight of a dragonfly, a bumblebee, and a cicada using the PIV system to identify the airflow generated by these wings.

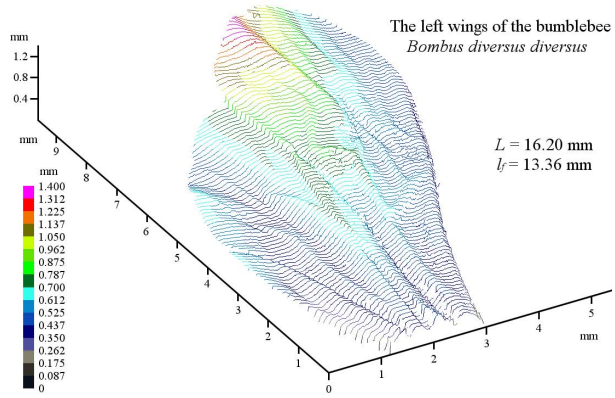

Fig. 9 The left forewing with hindwing of the bumblebee, *Bombus diversus diversus*

3.2.1 The flow around the flapping dragonfly

Figure 10 shows examples of the measurement results obtained by the PIV system. These figures show the distribution of velocity vectors around the dragonfly, *Orthetrum triangulare melania* ($L = 49.26$ mm, $l_f = 42.44$ mm, $l_h = 40.40$ mm) in the tethered state. The measurement location was on the plane that was 15 mm from the center of the body ($y = 15.0$ mm). This measurement location was inside and near the nodus of the dragonfly. The airflow in the wind tunnel was uniform and flowed from the left side to right side of the figure. The uniform velocity was $U_0 = 2.27$ m/s in the experiments. Although the velocity vectors were displayed by red arrows, the range of velocity from 0 to 2.5 m/s was removed for easy observation of the airflow generated by the dragonfly. In these figures, white curved lines on the wings are shown using a light sheet of the Nd: YAG lasers, this illuminated a single wing section of the dragonfly. The distribution of velocity vectors in the motion of a descending forewing is shown in Fig. 10 (a), the distribution of velocity vectors in the motion of an ascending hindwing is shown in Fig. 10 (b), and the distribution of velocity vectors in the motion of an ascending

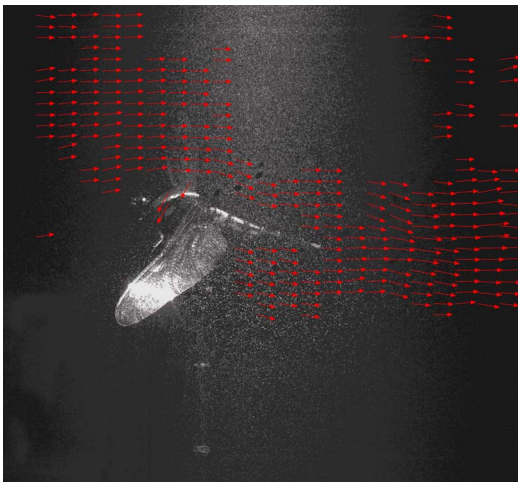

(a) Descending forewing

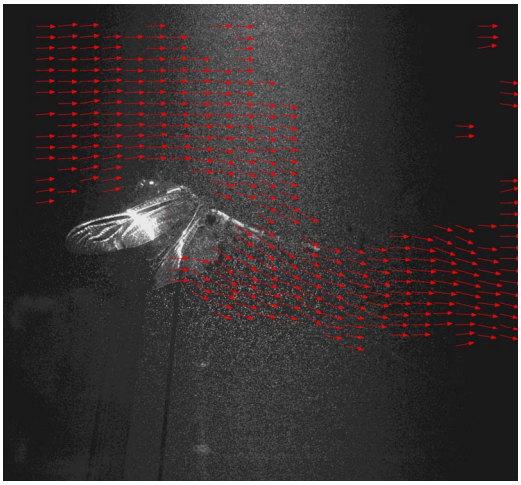

(b) Ascending hindwing

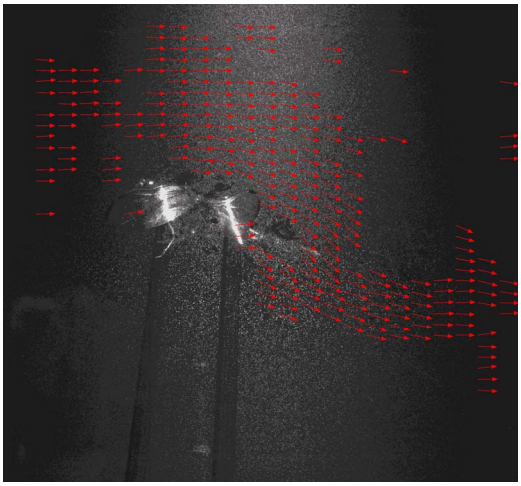

(c) Ascending forewing with hindwing

Fig. 10 The distribution of velocity vectors around the dragonfly, *Orthetrum triangulare melania* ($L = 49.26$ mm, $l_f = 42.44$ mm, $l_h = 40.40$ mm, $U_0 = 2.27$ m/s, $y = 15.0$ mm)

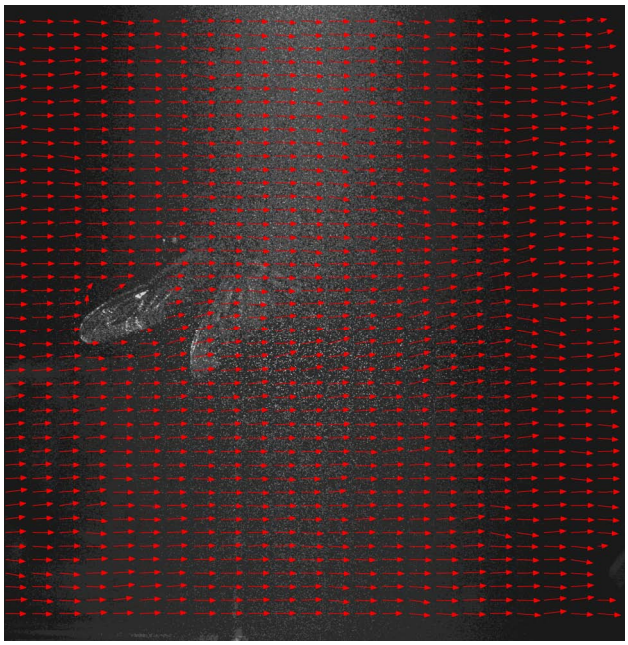

Fig. 11 The distribution of velocity vectors around the dragonfly, *Orthetrum triangulare melania* ($L = 49.26$ mm, $l_f = 42.44$ mm, $l_h = 40.40$ mm, $U_0 = 2.27$ m/s, $y = 35.0$ mm)

forewing with hindwing is shown in Fig. 10 (c). From these figures, the red arrows indicated that the airflow moves smooth and fast from above the thorax to the back of the tail. The flapping of the forewing with the hindwing always forced downward airflow backwards. Thus, we can see how the wing generates the required thrust for flapping flight.

Figure 11 shows the distribution of velocity vectors around the same dragonfly at the measurement plane $y = 35.0$ mm. The measurement location was near the tip of the wings. Insect wings move through three-dimensional tracks during flapping, and the wings are formed into a three-dimensional shape. Insects make very complex airflows around flapping wings during flight. In the figure, such special airflows were not observed near the wingtips. It can be seen that although the dragonfly wings made airflows for flight, the airflows near the wingtip were weaker than the airflows near the center of the wings. That is, this fact suggests the wingtip has some role in controlling to flight, and does not have a

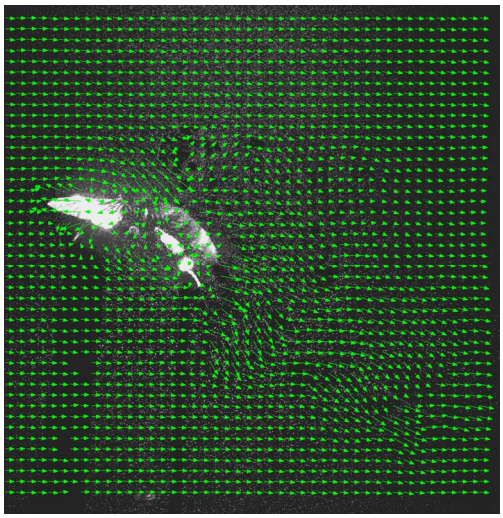

(a) Distribution of velocity vectors

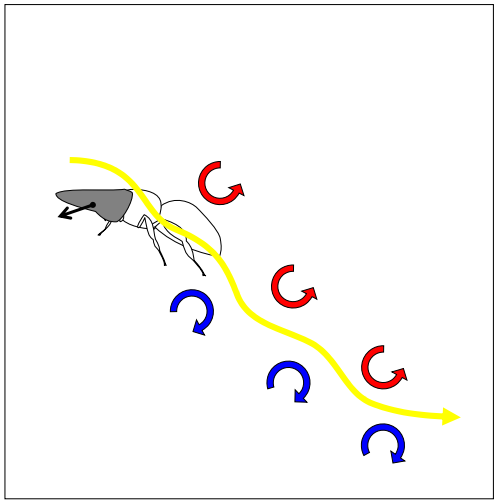

(b) Direction of the flow

Fig. 12 The flow fields around the bumblebee, *Bombus ignitus* for the descending wing ($L = 15.72$ mm, $l_f = 15.01$ mm, $U_0 = 2.33$ m/s, $y = 9.0$ mm)

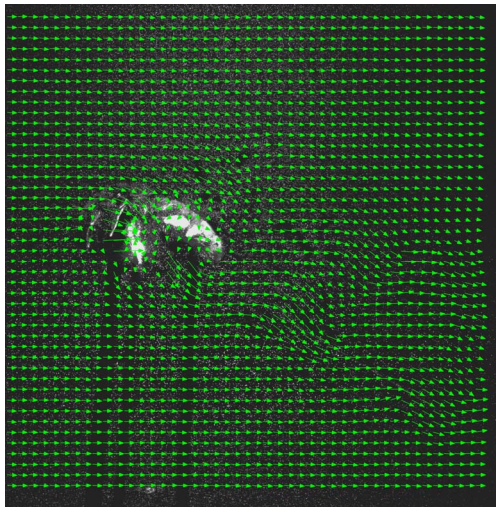

(a) Distribution of velocity vectors

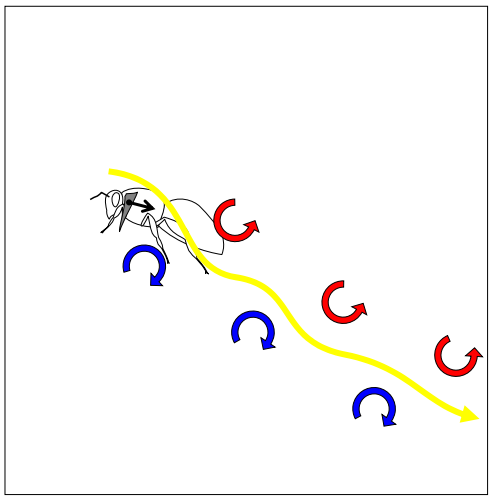

(b) Direction of the flow

Fig. 13 The flow fields around the bumblebee, *Bombus ignitus* for the ascending wing ($L = 15.72$ mm, $l_f = 15.01$ mm, $U_0 = 2.33$ m/s, $y = 9.0$ mm)

role in generating a lift force.

3.2.2 The flow around the flapping bumblebee

Figure 12 and 13 show the distributions of velocity vectors around the flapping wing of a tethered bumblebee, *Bombus ignitus* ($L = 15.72$ mm, $l_f = 15.01$ mm) in a uniform air velocity $U_0 = 2.33$ m/s at a plane for $y = 9.0$ mm. The distribution of velocity vectors in the motion of descending wings is shown in Fig. 12 (a), at the motion of ascending wings is shown in Fig. 13 (a). And, the direction of airflow was drawn as shown in Fig. 12 (b) and 13 (b). It can be observed that in a single flap that the descending wing generates a counterclockwise airflow (as drawn by the red arrow) and the ascending wing generates a clockwise flow (as drawn by the blue arrow). From these figures, we can see how the periodical vortex rings are generated in the flapping bumblebee [2]. The airflow moved in direction of the yellow

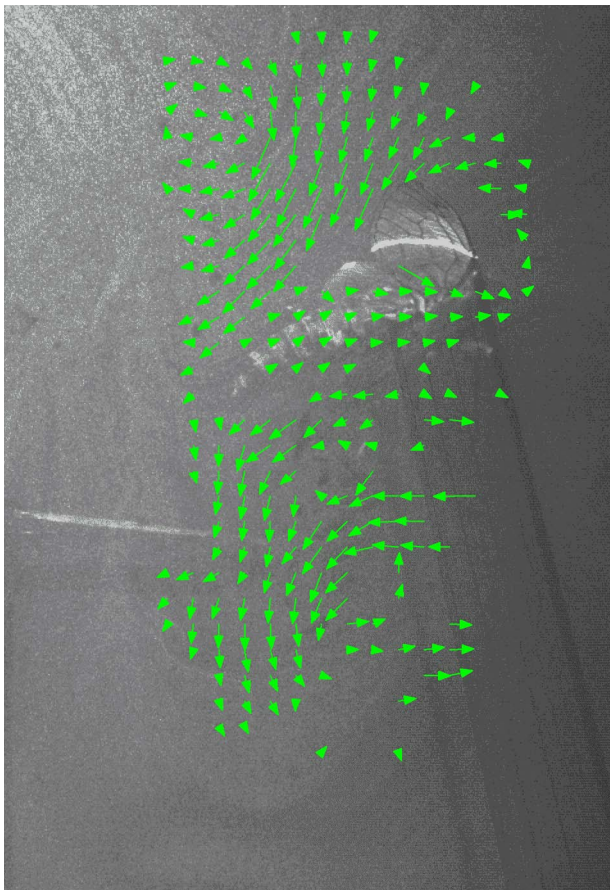

Fig. 14 The distribution of velocity vectors around the cicada, *Meimuna opalifera* to take off ($L = 27.54$ mm, $l_f = 32.32$ mm, $U_0 = 0$ m/s)

arrow; starting above the thorax moving across the abdomen to the bottom of the tail.

3.2.3 The flow around the flapping cicada in free flight

Figure 14 shows the distributions of velocity vectors around the cicada, *Meimuna opalifera* ($L =$ 27.54 mm, $l_f = 32.32$ mm) in free flight in the box. This was measured by the experimental system shown in Fig. 2 (b). This figure shows the moment that the cicada descended its wings. Although it can not be observed the line of vortex rings is similar to the bumblebee flapping, one clockwise vortex was shown over the cicada and one weak counterclockwise vortex under the cicada. At this time, there was a high velocity field from 2.0 to 2.7 m/s above the thorax. It was also observed in the moment following Fig. 14 that the airflows from the upper right to the lower left area under the flight route remained when the cicada had flown away. This also occurred in the case of the bumblebee. This suggests that the upper vortex generated during lifting shifted downward and was blown out by the lower vortex that was generated for forward thrust.

4 Summary

The wing morphology of these insects and the velocity fields around their flapping wings have been studied using two experimental apparatuses. The results of the studies are summarized as follows.

Surface roughness of the wing of the dragonfly, cicada and bumblebee were visualized by the three-dimensional images. The dragonfly, *Sympetrum frequence* forewing performed three roles, the cicada, *Tanna japonensis japonensis* had a corrugated membrane on the forewing, and the bumblebee, *Bombus diversus diversus* transformed the shape of its wings for connecting the forewing with the hindwing.

The Velocity vectors around the flapping dragonfly, bumblebee and cicada were analyzed using the PIV system. Airflow around flapping dragonfly, *Orthetrum triangulare melania* always forced smooth and fast downwards and backwards, however the flow near the wingtip was inconspicuous. The flapping bumblebee, *Bombus ignitus* had generated the periodical vortex rings behind it. The observation of the vortex rings over the flapping cicada, *Meimuna opalifera* in free flight was successful.

References

[1] Azuma, A.: *The Biokinetics of Flying and Swimming*, Springer-Verlag, 1992.

[2] Brodsky, A. K.: *The Evolution of Insect Flight*, Cambridge Univ. Press, 1994.

[3] Wootton, R.: How flies fly, *Nature*, **400**(1999), pp. 112-113.

[4] Grodnitsky, D. L.: *Form and Function of Insect Wings*, The Johns Hopkins Univ. Press, 1999.

[5] Fearing, R. S., Chiang, K. H., Dickinson, M. H., Pick, D. L., Sitti, M. and Yan, J.: Wing transmission for a micromechanical flying insect, *Proceedings of the 2000 IEEE International Conference on Robotics & Automation*, (2000), pp. 1509-1516.

[6] Michelson, R. C. and Reece, S.: Update on flapping wing micro air vehicle research - ongoing work to develop a flapping wing, crawling "Entomopter", *13th Bristol International RPV/UAV Systems Conference Proceedings*, (1998), pp. 30.1 - 30.12.

[7] Sudo, S., Tsuyuki, K. and Tani, J.: Wing morphology of some insects, *JSME International Journal* Series C, **43**-4(2000), pp. 895-900.

[8] Somps, C. and Luttges, M.: Dragonfly flight: novel uses of unsteady separated flows, *Science*, **228**(1985), pp. 1326-1328.

[9] Ellington, C. P., Berg, C., Willmott, A. P. and Thomas, A. L. R.: Leading-edge vortices in insect flight, *Nature*, **384**(1996), pp. 626-630.

[10] Dickinson, M. H. and Gotz, K. G.: The wake dynamics and flight forces of the fruit fly (*drosophila melanogaster*), *The Journal of Experimental Biology*, **199**(1996), pp. 2085-2104.

[11] Okamoto, M., Yasuda, K. and Azuma, A.: Aerodynamic characteristics of the wings and body of a dragonfly, *The Journal of Experimental Biology*, **199**(1996), pp. 281-294.

[12] Sudo, S., Tsuyuki, K., Ito, Y. and Nishiyama, H.: On the functional design of a dragonfly wing, *Proceedings of the 1st International Symposium on Aqua Bio-Mechanisms/International Seminar on Aqua Bio-Mechanisms*, (2000), pp. 233-238.